Technetium-99m Dimercaptosuccinic Acid Scintigraphy Studies of Renal Cortical Scarring and Renal Length

Monica A. Rossleigh, Robert H. Farnsworth, Diane M. Leighton, James L.C. Yong, Margaret Rose and Caryl L. Christian
Departments of Nuclear Medicine, Pathology and Animal Care, Prince of Wales Hospital; Departments of Nuclear Medicine, Urology and Radiology, Sydney Children's Hospital; and Department of Urology, Prince Henry Hospital, Sydney, Australia

The aims of this study were to validate ^{99m}Tc-dimercaptosuccinic acid (DMSA) scintigraphy appearances with histopathological features of scarring; to evaluate the sensitivity and specificity of ^{99m}Tc-DMSA and ultrasound for the detection of renal scarring; to compare planar, pinhole and SPECT techniques when using ^{99m}Tc-DMSA; and to compare ^{99m}Tc-DMSA and ultrasound renal length measurement. **Methods:** Reflux nephropathy was induced in large white pigs using established methods. To ensure that the abnormalities detected were scars and not inflammatory changes, the pigs were not studied until 3 mo after the treated episode of acute pyelonephritis confirmed by ^{99m}Tc-DMSA. **Results:** Twenty pigs were enrolled in the study. Eleven reached the end point, but only nine pigs (18 kidneys) were available for analysis. Thirty-four scars were identified pathologically; 24 were present macroscopically and a further 10 were seen only on microscopy. Technetium-99m-DMSA abnormalities correlated with scars histopathologically with an accuracy of 92% versus that of ultrasound, 75% ($p < 0.001$). Technetium-99m-DMSA more accurately identified scarring with a higher sensitivity (76% versus 29%) and specificity (98% versus 92%) than ultrasound. On the ^{99m}Tc-DMSA study, pinhole imaging had the highest accuracy (92%) when compared with planar (90%) and SPECT (87%) data. These differences were not statistically significant. Renal lengths as measured on ^{99m}Tc-DMSA more closely correlated with length measurement at pathological examination than ultrasound. Technetium-99m-DMSA measurement was, on average, 6% higher than pathology, and ultrasound was, on average, 22% lower. **Conclusion:** Technetium-99m-DMSA appears to be the preferred method for the detection of renal cortical scarring and accurate renal length measurement when compared with ultrasound examination.

Key Words: technetium-99m dimercaptosuccinic acid; ultrasonography; pathology

J Nucl Med 1998; 39:1280–1285

Vesicoureteric reflux (VUR) is the most common congenital anomaly of the urinary tract. The detection of renal cortical scarring due to reflux nephropathy is important, as it can result in the later development of hypertension and chronic renal failure. In children with VUR, the choice of medical or surgical management may be influenced by the presence or absence of renal cortical scarring. Both ultrasound examination and ^{99m}Tc-dimercaptosuccinic acid (DMSA) scintigraphy are standard diagnostic techniques used clinically to evaluate kidneys for the presence of renal cortical scarring. Ultrasound is the initial investigation of choice when evaluating the renal tract, as it is readily available, easy to perform and does not involve the use of ionizing radiation. Several clinical studies have concluded that ^{99m}Tc-DMSA is more sensitive for detecting renal cortical scars (*1–4*). However, ^{99m}Tc-DMSA does involve the administration of a radioactive material and is less widely available than ultrasound.

The aims of this study were to use an experimental animal model to correlate ^{99m}Tc-DMSA appearances with histopathological features of renal cortical scarring; to evaluate the sensitivity and specificity of ^{99m}Tc-DMSA and ultrasound for the detection of renal cortical scars; to compare planar, pinhole and SPECT techniques when using ^{99m}Tc-DMSA to determine their sensitivity in detecting renal cortical scars; and to compare ^{99m}Tc-DMSA and ultrasound in the measurement of renal length.

MATERIALS AND METHODS

Approval for this study was obtained from Animal Care and Ethics Committee of University of New South Wales.

The pig is an established experimental model for the assessment of VUR and pyelonephritis (*5–11*). It is the only large animal possessing a multipapillary kidney with compound papillae, which allows intrarenal reflux to occur in the presence of VUR.

Twenty large white pigs were studied, of which nine reached the end of the protocol. The flow chart (Fig. 1) outlines the protocol used. Four- to 6-wk-old male piglets were fed standard diets and were allowed to acclimatize to the animal holding facility of this institution for 1 wk. Baseline ^{99m}Tc-DMSA studies were performed in all pigs to confirm the presence of two normal kidneys. Unilateral VUR was then induced surgically. A low midline incision was made to expose the urinary bladder. The bladder was opened, and VUR was achieved by making an incision from the roof of the intravesical ureter from the ureteric orifice to the ureterovesical junction, thus laying open the submucosal ureteric tunnel. The other ureter was left intact as a control. The bladder was stitched to the anterior abdominal wall to facilitate future suprapubic puncture. One week later, the pig was again anesthetized, and ionic iodine contrast was introduced into the urinary bladder via a suprapubic catheter for an x-irradiation cystogram to confirm the presence of VUR (Fig. 2). If VUR was achieved, 10 ml of a standardized concentration broth of *Eschericha coli*, followed by an 8-ml ball of molten wax, which acted as a foreign body nidus, was then inserted into the bladder to induce pyelonephritis. The same strain and concentration of *E. coli* were used in all pigs. The *E. coli* was obtained originally from an infant who had a severe episode of acute pyelonephritis caused by this organism. An overnight culture of *E. coli* broth was used. One week later, a ^{99m}Tc-DMSA study was performed to determine whether acute pyelonephritis was established (Fig. 3). Once pyelonephritis was confirmed, the wax ball was removed surgically and the pig was placed on oral amoxicillin for 7 days.

To ensure that the abnormalities detected were scars and not inflammatory changes, the pigs were not studied until 3 mo after the treated episode of acute pyelonephritis. At that time, the pigs

Received May 13, 1997; revision accepted Oct. 13, 1997.
For correspondence or reprints contact: Monica A. Rossleigh, FRACP, Chairman, Department of Nuclear Medicine, Prince of Wales Hospital, High Street, Randwick NSW 2031, Sydney, Australia.

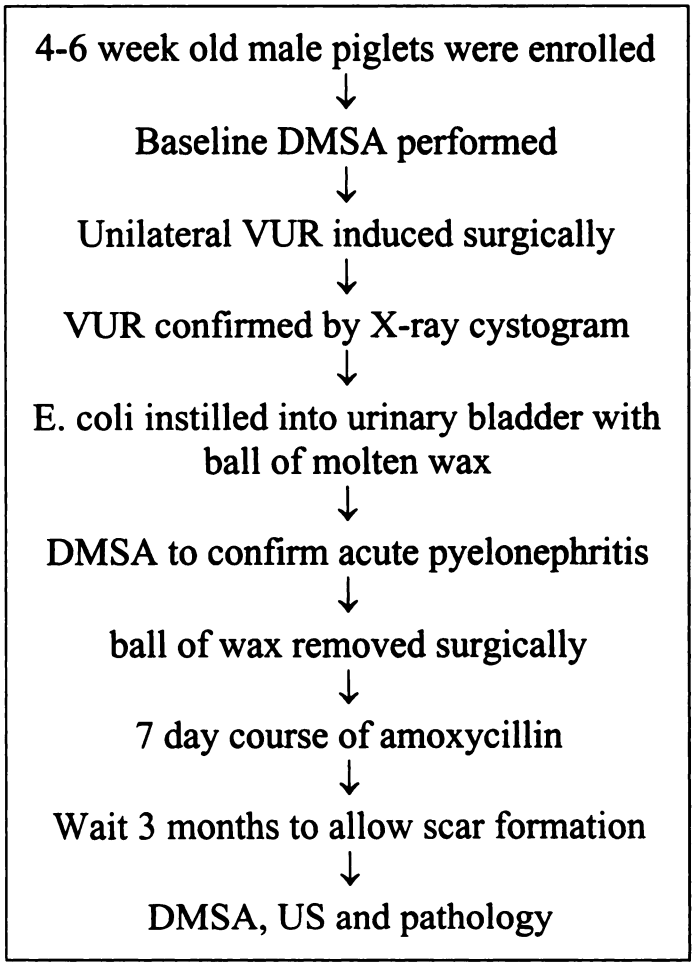

FIGURE 1. Flow chart of study protocol.

underwent an ultrasound examination and a ^{99m}Tc-DMSA study comprised of planar, pinhole and SPECT imaging, all under general anesthesia. Halothane, nitrous oxide and oxygen were given via a mask. Once all imaging had been acquired, a lethal dose of barbiturate was administered intravenously and the kidneys then were removed postmortem. The kidneys were placed in formalin for later pathological examination.

Technetium-99m-DMSA Scintigraphy

The final ^{99m}Tc-DMSA study was undertaken on a GE 400 AC single-head gamma camera (General Electric, Milwaukee, WI) connected to a Starcam computer, at least 3 hr after the intravenous injection of 200 to 300 MBq ^{99m}Tc-DMSA. This larger dose was required, as the pigs weighed approximately 120 kg at the end point of the study, and the pigs were often imaged 4 to 6 hr postinjection. Imaging of the pigs was undertaken when all clinical studies for the day had been completed. This resulted in varying times between injection and imaging of the pigs. Posterior planar images were performed using a high-resolution, parallel-hole collimator; posterior pinhole images were obtained using a pinhole collimator with a 3-mm aperture. SPECT images were acquired using a 180° circular orbit at 3° angles and 30 sec of scanning time per stop. The SPECT studies were reconstructed using a Butterworth filter, and attenuation correction was applied. The slices were displayed in coronal, sagittal and transaxial planes, and each slice was 1 pixel wide. Because of the large size of the pigs and difficulty maintaining an open airway in the supine position, the pigs were imaged lying on their side (Fig. 4). Renal lengths were measured on the planar DMSA study only, by assessing the maximum pixel length and then converting this to centimeters.

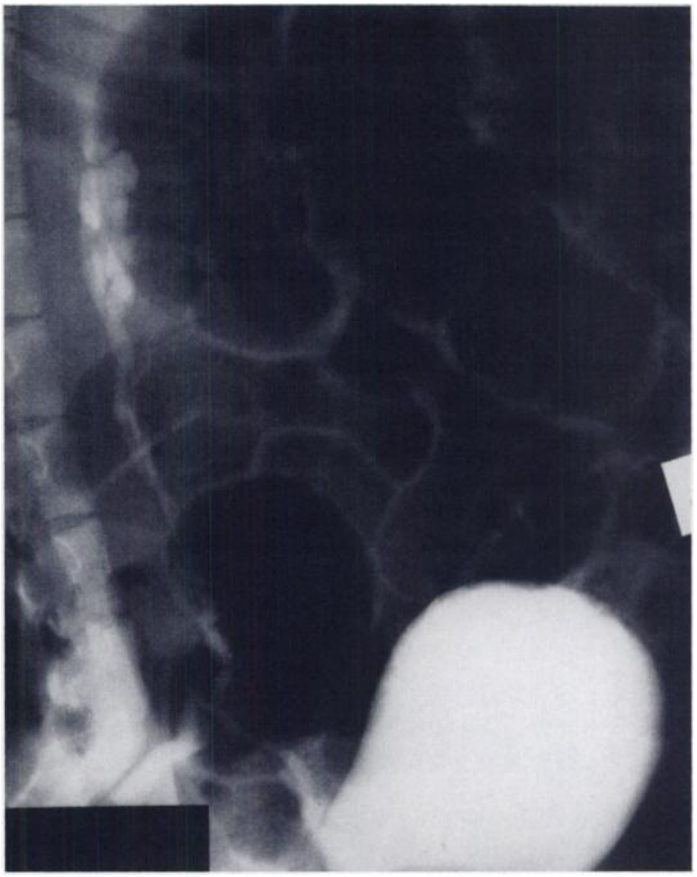

FIGURE 2. Cystogram confirming successful surgical induction of vesicoureteric reflux.

As in the clinical setting, a ^{99m}Tc-DMSA study was considered abnormal when there was significant reduction in renal function, as assessed by differential function measurements and/or decreased or absent uptake of tracer in the renal cortex, causing distortion or

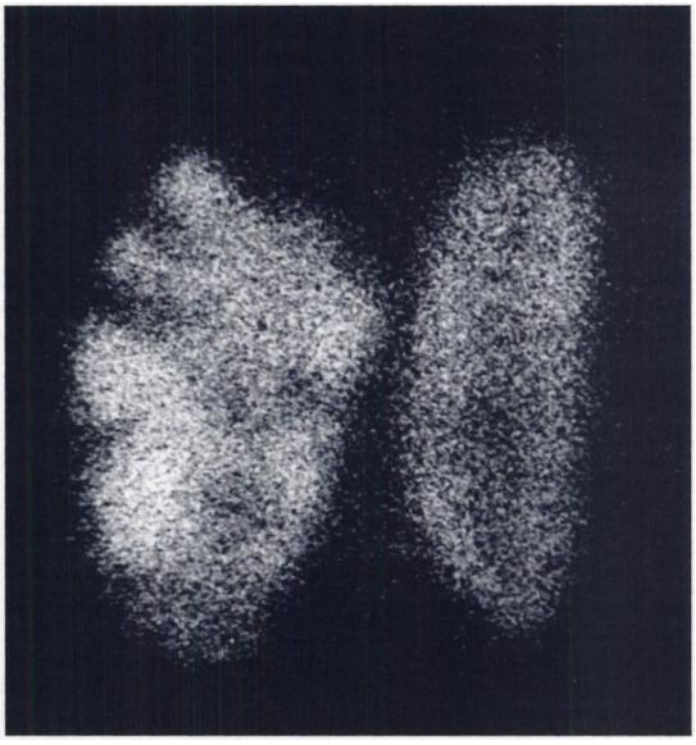

FIGURE 3. Technetium-99m-DMSA study confirming presence of experimentally induced multifocal pyelonephritis of left kidney. Contralateral control kidney has normal appearance.

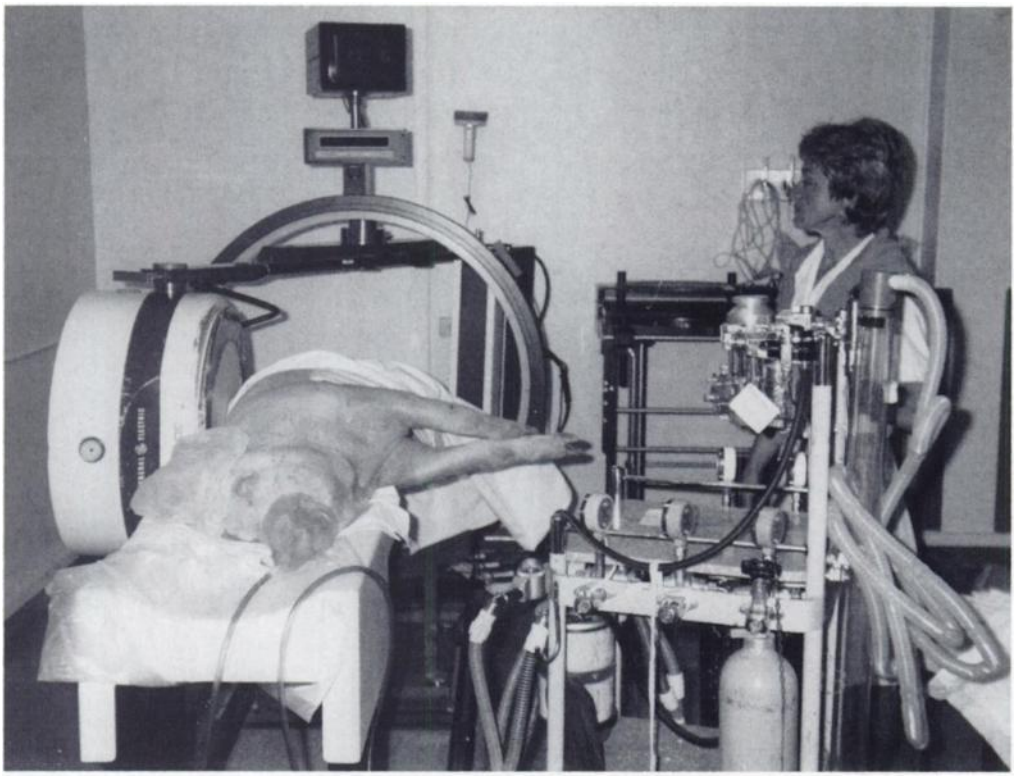

FIGURE 4. Pig (120 kg) undergoing final DMSA study under general anesthesia.

indentation of the normal renal outline. All of the ^{99m}Tc-DMSA studies were reported by the nuclear medicine physician.

Ultrasound Studies

Ultrasound studies were undertaken using an Acuson 128 real-time ultrasound machine and a 3-MHz transducer, with the pig lying on its side. The animal was rotated for imaging of both kidneys. All of the ultrasound studies were reported by the radiologist.

An ultrasound was considered abnormal if it exhibited focal or segmental reduction of parenchymal thickness, assessed by direct visualization and measurement of the parenchyma from the renal outline to the collecting system and/or dilatation of renal calyces and/or overall reduction of kidney length relative to the contralateral kidney. The maximum renal length was measured on the coronal plane using a standardized technique.

Pathological Examination

The kidneys were removed at autopsy, and a stitch was inserted into the capsule to identify the upper pole. The kidneys were then placed immediately in a large volume of 10% buffered formalin and bisected as soon as they were received in the pathology department and further fixed for at least 48 hr. After fixation, each kidney was weighed, measured and examined for scarring and other abnormalities. The site and size of each scar were recorded on a kidney map. Blocks of tissues were selected for light microscopic study from scarred and relatively normal-looking areas.

Macroscopic examination showed that the size of cortical scars varied considerably. Cortical scars had a typical V-shaped appearance on cut surface with the broad base directed toward the capsule and the apex toward the medulla. The scarred cortex had a characteristic contracted or depressed area on the capsule. There were no cystic changes macroscopically.

Microscopically, the changes found were typical of those seen in chronic pyelonephritis (chronic tubulointerstitial nephritis). There was contraction of renal parenchyma at the site of scarring. Many tubules were lost or atrophic and sometimes slightly dilated or cystic. The interstitium was fibrotic, with varying degrees of chronic inflammation. There was also complete loss of glomeruli in scarred areas; those that remained showed periglomerular fibrosis and tuft atrophy with dilatation of Bowman's space.

Separate kidney maps were used by the nuclear medicine physician, radiologist and pathologist for each to draw in where the scars were detected by each modality, and the lengths of all kidneys were recorded. Each kidney was divided into seven regions: upper pole—medial, apex and lateral, midzone, and lower pole—medial, apex and lateral. The ^{99m}Tc-DMSA, ultrasound and pathology data were analyzed separately by different authors without knowledge of the others' findings. In this way, an objective assessment and comparison could be undertaken.

RESULTS

Twenty large white pigs were enrolled in the study, of which 11 reached the end point. The reasons for nine pigs not reaching the end point were as follows:

1. Infective complications/sepsis (n = 5). These pigs became too ill and passed the predetermined end point and were euthanized;
2. No VUR demonstrated (n = 3); and
3. No induction of pyelonephritis (n = 1).

In addition, the kidneys of two pigs that reached the end point were lost before pathological examination was undertaken. This left nine pigs (18 kidneys) available for analysis. Three pigs (6 kidneys) that did not reach the end point had their kidneys removed for histological evaluation, and no VUR was demonstrated in two and failure of induction of pyelonephritis occurred in one. No renal cortical scars or other anatomical abnormalities were found. These pigs constituted shams in this experiment. Thirty-four scars were induced in this study. The analysis of the scars is summarized in Table 1. Ten were identified microscopically only, and 24 were identified both microscopically and macroscopically. Eight of these scars were not identified by any of the four imaging methods (i.e., planar, pinhole, SPECT and ultrasound), and all of these undetected scars were only identified microscopically. Eight of 92 sites not scarred pathologically were designated as scarred by one or

TABLE 1
Number of Sites Correctly Categorized According to Imaging Method

	Pathology category				
	No scars	Microscopic scars	Macroscopic scars	All scars	All sites
No. of sites in each pathology category	92	10	24	34	126
Planar DMSA	92	2	19	21	113
Pinhole DMSA	91	2	23	25	116
SPECT DMSA	90	2	18	20	110
Ultrasound	85	0	10	10	95

more of the four methods, i.e., false-positive results. Of these eight false-positives, six were incorrectly called scars by ultrasound alone; one by SPECT alone; and one by pinhole, SPECT and ultrasound. Of the 24 macroscopically scarred sites, planar failed to identify 5, SPECT did not identify 6 and pinhole did not identify 1, compared with 14 macroscopic scars not visualized by ultrasound.

In the comparison of the different methods used on the ^{99m}Tc-DMSA study (Table 2), pinhole imaging had the highest accuracy (92%) when compared with planar (90%) and SPECT (87%). The accuracy of combining the methods, i.e., planar + pinhole, planar + SPECT and planar + pinhole + SPECT, were all the same at 92%.

Statistical analysis is outlined in Table 3. Technetium-99m-DMSA abnormalities correlated with scars histopathologically with an accuracy of 92% compared with ultrasound with an accuracy of 75%. Using the McNemar test, this is a statistically significant difference of $p < 0.001$. Technetium-99m-DMSA more accurately identified scarring with a higher sensitivity (76% versus 29%) and specificity (98% versus 92%) than ultrasound (Fig. 5). There was no statistically significant difference demonstrable between planar, pinhole and SPECT ^{99m}Tc-DMSA scintigraphy.

The renal length, as measured on ^{99m}Tc-DMSA planar scintigraphy and on ultrasound examination, was compared to length measurement at pathological examination. The mean ± s.d. length on pathology was 12.7 ± 1.7 cm, on ^{99m}Tc-DMSA was 13.5 ± 1.7 cm and on ultrasound was 10.1 ± 2 cm. The ^{99m}Tc-DMSA measurement was, on average, 6% higher than pathology, and the ultrasound measurement was, on average, 22% lower (Fig. 6).

DISCUSSION

There have been several previous studies in which ^{99m}Tc-DMSA has been correlated with acute pyelonephritis in the pig model (*7–11*). This project was aimed at the detection of

TABLE 2
Number of Sites Categorized According to Combination of DMSA Methods

	Pathology category				
	No scars	Microscopic scars	Macroscopic scars	All scars	All sites
No. of sites in each pathology category	92	10	24	34	126
Planar	92	2	19	21	113
Planar + pinhole	91	2	23	25	116
Planar + SPECT	90	3	23	26	116
Planar + pinhole + SPECT	90	3	23	26	116

TABLE 3
Sensitivity, Specificity, Positive Predictive Probability (PPP) and Negative Predictive Probability (NPP) of Imaging Methods (%)

	Sensitivity	Specificity	PPP	NPP	Overall accuracy
Planar	62	100	100	88	90
Pinhole	74	99	96	91	92
SPECT	59	98	91	87	87
Ultrasound	29	92	59	78	75
Planar + pinhole	74	99	96	91	92
Planar + SPECT	76	98	93	92	92
Planar + pinhole + SPECT	76	98	93	92	92

chronic renal cortical scarring with no acute inflammatory component. Lesions due to acute pyelonephritis are usually larger and are often transient (*12*). We decided to wait 3 mo from the acute pyelonephritis, which was treated with antibiotics, before undertaking the final imaging, so that only scars would be visualized. This decision resulted in logistic problems, as the pigs weighed ~120 kg at the end point of the study, necessitating imaging with them on their sides.

This study has confirmed that abnormalities detected on ^{99m}Tc-DMSA performed at least 3 mo after a treated urinary tract infection do correspond with sites of renal cortical scarring. Previous animal data using the pig model have confirmed the ^{99m}Tc-DMSA appearances of acute pyelonephritis (*7–11*). Arnold et al. (*9*) did demonstrate ^{99m}Tc-DMSA findings in pigs with renal scarring, but his pigs were scanned 7–21 days after the induced urinary tract infection, which was ongoing. There were no acute inflammatory or infective changes in the pigs enrolled in this study because of the 3-mo period between the treated urinary tract infection and the ^{99m}Tc-DMSA study.

This study has confirmed the higher accuracy of ^{99m}Tc-DMSA in the detection of renal cortical scarring when compared with ultrasound. This upholds clinical studies with similar findings. Several articles have reported greater sensitivity with DMSA compared with ultrasound for the detection of either acute pyelonephritis or renal cortical scarring (*1–4,13–16*). However, it must be acknowledged that the ultrasound obtained in this study was limited by the large size of the pigs and the large amount of bowel gas present.

There has been much debate in the literature as to the optimal methods to be used when ^{99m}Tc-DMSA is performed (*17–20*). Parallel-hole planar imaging is essential for differential renal function calculation. This is important information that cannot be obtained with pinhole or SPECT acquisition. The question is then whether to add pinhole or SPECT to the planar image to improve scar detection. In this study, pinhole appears superior to SPECT. However, the SPECT studies performed in this investigation were not technically optimal because of the large size of the pig at the time of the ^{99m}Tc-DMSA study. There was significant anterior attenuation because of their size and weight. The pinhole images were easier to obtain. Majd et al. recently compared pinhole and SPECT imaging in the detection of experimental acute pyelonephritis in piglets (*11*). They found the accuracy to be the same. However, they favored pinhole imaging because of the higher technical intervention required in both acquiring and analyzing SPECT data. In addition, any patient movement necessitates the SPECT study being acquired from the beginning again, whereas pinhole imaging is more easily repeated. Connolly et al. (*20*) also advocate the addition of pinhole or SPECT imaging to planar imaging to improve the detection of renal cortical scarring by ^{99m}Tc-DMSA. In our

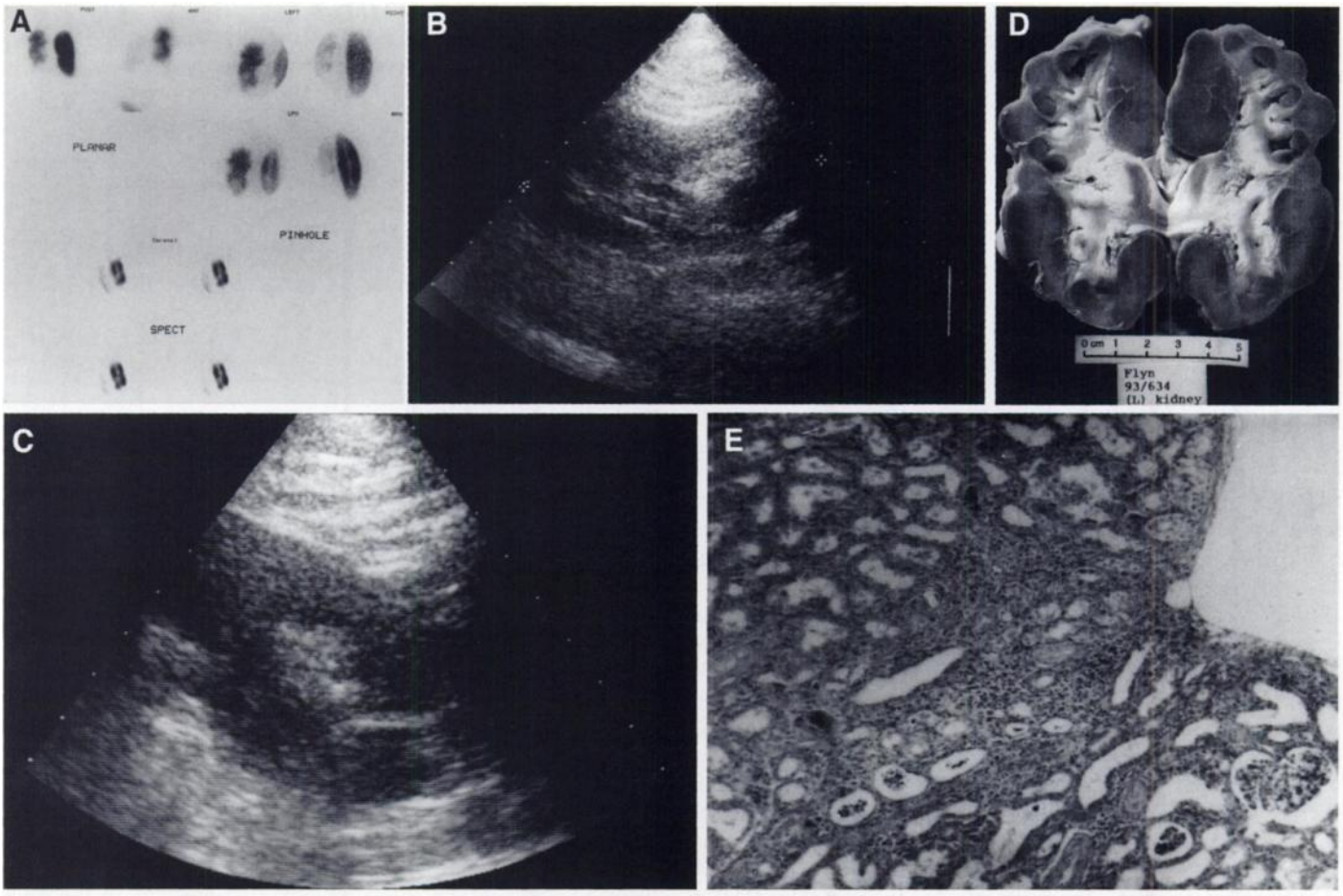

FIGURE 5. (A) Planar, pinhole and coronal slices of SPECT DMSA study confirming presence of extensively scarred left kidney. (B) Ultrasound examination of left kidney of same pig (sagittal view with no scars apparent). (C) Ultrasound examination of left kidney (transverse view demonstrating scarring in upper pole only). (D) Pathological specimen confirming presence of multiple macroscopic scars in left kidney involving upper and lower poles as well as midzone. (E) Microscopic evidence of scarring in left kidney: contraction of renal parenchyma, tubular and glomerular loss and fibrotic interstitium.

experience, we would support the use of planar and pinhole images as the optimal combination when performing ^{99m}Tc-DMSA for renal cortical scarring detection. However, we were unable to demonstrate a statistically significant difference between planar, pinhole and SPECT ^{99m}Tc-DMSA scintigraphy in this study. Apart from the technical considerations associated with SPECT, as outlined by Majd, there is also the problem of false-positive defects due to normal variants, such as the inter-renicular septum, identified only on SPECT (*21,22*).

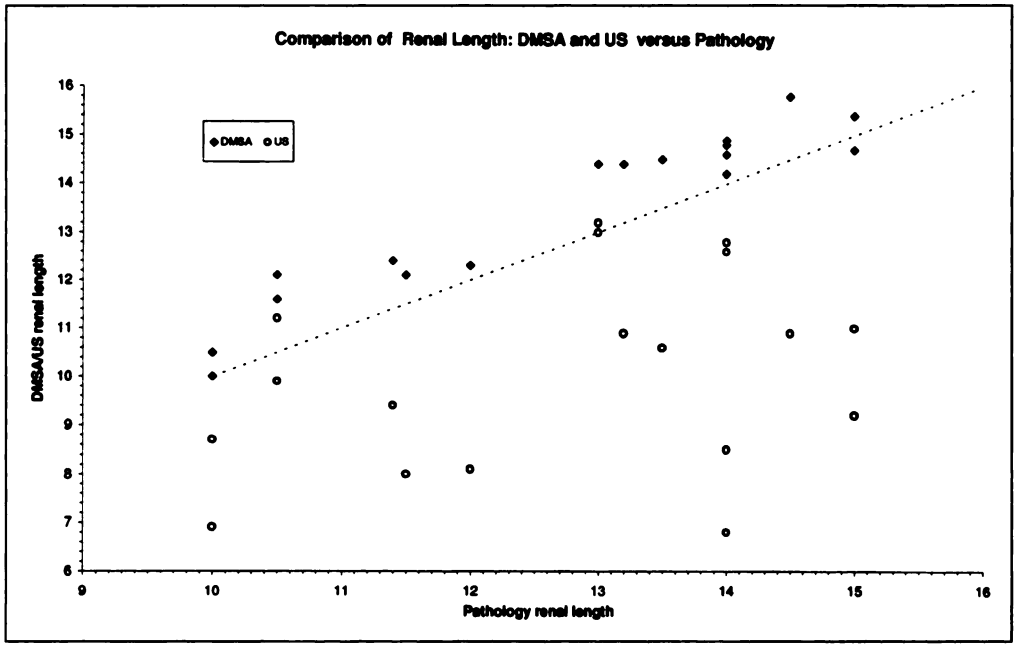

FIGURE 6. Graph comparing renal lengths as measured by ultrasound and DMSA with pathology.

Renal length appears to be more accurately measured on ^{99m}Tc-DMSA than on ultrasound examination. The ^{99m}Tc-DMSA measurement was, on average, 6% higher than pathology. This can be attributed to the lack of blood within the kidneys at the time of pathological examination, which was undertaken several months after the autopsy, with the kidney having been placed in formalin. In vivo, it is highly likely that the pigs' kidneys would have been longer. Ultrasound measurement on this study appeared to underestimate renal length significantly when compared with pathology, and there was a wider s.d., indicating a greater variability in measurements. The ultrasound was technically difficult in these animals because of their large size and the large amount of bowel gas present, and because they were anesthetized but not intubated and ventilated. Thus, images taken at full inspiration could not be obtained. When performed clinically, patients are asked to hold their breath on full inspiration so that the full length of the kidney can be imaged. However, it can be difficult to obtain the maximum longitudinal axis reliably. The overall longer length measured on ^{99m}Tc-DMSA when compared with ultrasound has been demonstrated previously using clinical data (*23*).

CONCLUSION

Technetium-99m-DMSA appearances have been correlated with histopathological features of renal cortical scarring in the pig model. Technetium-99m-DMSA has a significantly higher accuracy than ultrasound for the detection of renal cortical scars. A statistically significant difference between planar, pinhole and SPECT ^{99m}Tc-DMSA scintigraphy for the detection of renal cortical scarring could not be demonstrated in this study. Technetium-99m-DMSA appears to measure renal length more accurately than ultrasound, as the maximum longitudinal renal axis can be more reliably obtained.

ACKNOWLEDGMENTS

We thank Dr. Andrew Rosenberg for his help in setting up the protocol for this study; Dr. John Tapsall, Department of Microbiology, Prince of Wales Hospital, for providing the *E. coli* used in this study; Dr. Richard Fisher for his statistical analysis of the data; and Wayne Roach and Craig Weston for help with handling the large animals. We thank the Department of Medical Illustration, Prince of Wales Hospital, for reproducing the figures in this work and Jan Newman and Beverly Boas for secretarial assistance. This study was funded by research grants from the Australian Kidney Foundation and the Prince of Wales Children's Hospital Foundation.

REFERENCES

1. Farnsworth RH, Rossleigh MA, Leighton DM, Bass SJ, Rosenberg AR. The detection of reflux nephropathy in infants by technetium-99m dimercaptosuccinic acid studies. *J Urol* 1991;145:542–546.
2. Shanon A, Feldman W, McDonald P, et al. Evaluation of renal scars by technetium-labelled dimercaptosuccinic acid scan, intravenous urography and ultrasonography: a comparative study. *J Pediatr* 1992;120:399–403.
3. Tasker AD, Lindsell DR, Moncrieff M. Can ultrasound reliably detect renal scarring in children with urinary tract infection? *Clin Radiol* 1993;47:177–179.
4. Yen TC, Chen WP, Chang SL, Huang YC, Hsieh CP, Yeh SH, Lin CY. A comparative study of evaluating renal scars by ^{99m}Tc-DMSA planar and SPECT renal scans, intravenous urography, and ultrasonography. *Ann Nucl Med* 1994;8:147–152.
5. Hodson CJ, Maling TMJ, McManamon PJ, Lewis MG. The pathogenesis of reflux nephropathy (chronic atrophic pyelonephritis). *Br J Radiol* 1975;13(suppl):1–26.
6. Ransley PG, Risdon RA. Reflux and renal scarring. *Br J Radiol* 1978;14(suppl):1.
7. Rushton HG, Majd M, Chandra R, Yim D. Evaluation of technetium-99m-dimercaptosuccinic acid renal scans in the detection and localization of experimental acute pyelonephritis in piglets. *J Urol* 1988;140:1169–1174.
8. Parkhouse HG, Godley ML, Cooper J, Risdon RA, Ransley PG. Renal imaging with ^{99m}Tc-labelled DMSA in the detection of acute pyelonephritis: an experimental study in the pig. *Nucl Med Commun* 1989;10:63–70.
9. Arnold AJ, Brownless SM, Carty HM, Riskwood AMK. Detection of renal scarring by DMSA scanning: an experimental study. *J Pediatr Surg* 1990;25:391–393.
10. Giblin JG, O'Connor KP, Fildes RD, et al. The diagnosis of acute pyelonephritis in the piglet using single photon emission computerized tomography dimercapto succinic acid scintigraphy: a pathological correlation. *J Urol* 1993;150:759–762.
11. Majd M, Rushton HG, Chandra R, Andrich MP, Tardif CP, Rashti F. Technetium-99m-DMSA renal cortical scintigraphy for the detection of experimental acute pyelonephritis in piglets: comparison of planar (pinhole) and SPECT imaging. *J Nucl Med* 1996;37:1731–1734.
12. Rosenberg AR, Rossleigh MA, Brydon MP, Bass SJ, Leighton DM, Farnsworth RH. Evaluation of acute urinary tract infection in children by dimercaptosuccinic acid scintigraphy: a prospective study. *J Urol* 1992;148:1746–1749.
13. Bjorgvinsson E, Majd M, Eggli KD. Diagnosis of acute pyelonephritis in children: comparison of sonography and ^{99m}Tc-DMSA scintigraphy. *Am J Roentgenol* 1991; 157:539–543.
14. MacKenzie JR, Fowler K, Hollman AS, et al. The value of ultrasound in the child with an acute urinary tract infection. *Br J Urol* 1994;74:240–244.
15. Yen TC, Chen WP, Chang SL, et al. Technetium-99m-DMSA renal SPECT in diagnosing and monitoring pediatric acute pyelonephritis. *J Nucl Med* 1996;37:1349–1353.
16. Rushton HG. The evaluation of acute pyelonephritis and renal scarring with technetium-99m-dimercaptosuccinic acid renal scintigraphy: evolving concepts and future directions. *Pediatr Nephrol* 1997;11:108–120.
17. Mouratidis B, Ash JM, Gilday DL. Comparison of planar and SPECT ^{99m}Tc-DMSA scintigraphy for the detection of renal cortical defects in children. *Nucl Med Commun* 1993;14:82–86.
18. Buscombe JR, Hilson AJW, Hall ML, Townsend CE, Clarke G, Ell PJ. Does three-dimensional display of SPECT data improve the accuracy of technetium-99m-DMSA imaging of the kidneys? *J Nucl Med Technol* 1995;23:12–17.
19. Cook GJR, Lewis MK, Clarke SEM. An evaluation of ^{99m}Tc-DMSA SPECT with three dimensional reconstruction in 68 patients with varied renal pathology. *Nucl Med Commun* 1995;16:958–967.
20. Connolly LP, Treves ST, Connolly SA, et al. Comparison between planar, pinhole and SPECT ^{99m}Tc-DMSA imaging for the detection of renal cortical defects [Abstract]. *J Nucl Med* 1995;36:32P.
21. Rossleigh MA. The inter-renicular septum: a normal variant seen on DMSA SPECT. *Clin Nucl Med* 1994;19:953–955.
22. De Sadeleer C, Bossuyt A, Goes E, Piepsz A. Renal technetium-99m-DMSA SPECT in normal volunteers. *J Nucl Med* 1996;37:1346–1349.
23. Sisayan RM, Rossleigh MA, Mackey DWJ. Normograms of renal length in children obtained from DMSA scintigraphy. *Clin Nucl Med* 1993;18:970–973.